Sensors & Transducers, Vol. 245, Issue 6, October 2020, pp. 76-82

Sensors & Transducers

Published by IFSA Publishing, S. L., 2020
http://www.sensorsportal.com

Investigation of the Absorption Lines of a Kr - Ne Mixture in the Near Infrared Region Detected by Opto-galvanic Spectroscopy

U. H. P. Fischer and M. Schröder
University Applied Sciences, Friedrichstr. 57, 38855 Wernigerode, Germany
Tel.: + 49 3943659 351, fax: + 49 3943659 5351
E-mail: ufischer@hs-harz.de

Received: 30 July 2020 /Accepted: 23 September 2020 /Published: 30 October 2020

Abstract: In this work the optical absorptions of the Krypton 84 1 s_2 - 2 p_8 between 1270-1640 nm are analyzed to be used for an optical wavelength standard in this regime. The spectrum was measured using opto-galvanic spectroscopy which shows higher sensitivity than direct optical absorption spectroscopy. More than 30 usable absorption lines have been determined. Here, all absorption lines of the Krypton / Neon mixed gas were summarized which can be used in the transmission range of 1270 nm to 1640 nm. Additionally, a wavelength drift of the detected lines was measured using a climate chamber between 10°C and 50°C. Combining the Galvatron absorption of Kr lines with active feedback to a multi-channel laser comb source, we propose this system to be used as a secondary reference source for the calibration of spectral analyzers or in optical WDM networks.

Keywords: Wavelength Division Multiplex Systems WDM, Optical wavelength references, Optical networks, Opto-galvanic spectroscopy.

1. Introduction

Optical communication systems are since the last 30 years the backbone of all international data and telecom communications. Up to now, more than 10 Tbit/s can be distributed via one optical fiber in long-haul systems. This was realized by the use of highly parallel multi-channel transmission via many colors, called Wavelength Division Multiplex (WDM). Here, the International Telecommunication Union specified the channel location into a frequency space grid with 100/25 GHz distance in the infrared regime from 1300 nm to 1640 nm. To avoid interference between these densely arranged transmission channels, each transmitter output frequency has to be stabilized exactly in its center frequency to others. To supervise and stabilize the transmission comb, absolute frequency standards are very helpful to be integrated into optical cross-connect stations. Using excited state absorption lines of a Nobel gas is an easy way to generate reference frequencies, because these states are very stable and very small in linewidth. A well-known method is the detection of the absorption by the opto-galvanic effect (OGE). Here, a tube is filled with the gas Kr and the detection of the absorption will be performed by an electrical signal of the absorption cell via electrodes with high voltage supply. Many atomic transitions are nearby to the ITU grid frequencies of ITU G 652 Recommendation.

2. Wavelength Standards

Nowadays, atomic and molecular absorption lines are used in wide areas of optics as wavelength calibration references, since these form highly stable frequency standards even under fluctuating environmental conditions. Molecules such as acetylene and hydrogen cyanide have very narrow-band absorptions in the range of 1500 nm as rotation-vibration transitions. These transitions can easily be detected directly by absorption spectroscopy. Atomic transitions of noble gases in the range of 1300-1700 nm are generally not directly detectable, since they are transitions between excited states of the atom. These excitation states are usually formed with the aid of laser excitation or by means of an electrical gas discharge. A single gas laser reference line from the HeNe laser at 1523 nm can be used. Further atomic or molecular references can only be achieved by doubling the frequency of the light from e.g. Rubidium from 1560 nm to 780 nm can be achieved, which can only be achieved with very high expenditure on equipment [1-3].

In the case of an optical transition of an excited electronic state, it is assumed that the energy levels W_1 and W_2 are precisely delimited and that light absorption or emission only takes place with the transition frequency f_{12}. In fact, however, a blurring occurs due to various influences in the frequencies. A distinction is made between homogeneous and inhomogeneous line broadening. The homogeneous line broadening is caused by spontaneous emissions and collisions in gases or lattice vibrations in solids; the effect is the same for all atoms. An example of inhomogeneous line broadening is Doppler broadening, in which the frequency depends on the speed of the atoms. These effects are explained in more detail below.

The natural line width is a homogeneous broadening which depends on the lifetime τ of the levels involved. According to Heisenberg's uncertainty principle, the levels have the natural latitude ΔW.

The collision broadening is caused by the elastic collisions between the gas particles. It is also called pressure broadening because the number of impacts increases with pressure. These collisions change the phase of the emitted wavelength. A Fourier analysis of the resulting wave trains also gives a Lorentz profile. The half-width Δfs results from the mean time between the collisions τs. The resulting collision broadening is therefore proportional to the gas pressure and normally much larger than the natural line width Δfn. For a He-Ne laser, this is $\Delta fn \approx 10$ MHz and $\Delta fs = 100$ MHz.

The inhomogeneous Doppler broadening is caused by the frequency shift that is caused by the movement of the atoms or molecules.

The frequency depends on the direction of movement of the particle (1):

$$f'_{12} = f_{12}\left(1 \pm v/c\right) \tag{1}$$

According to Maxwell's velocity distribution, each particle has a different velocity v in thermal equilibrium. The result is the line shape $F_D(f)$ with a Gaussian profile. With the same half-width Δf_D, (2) this falls more steeply than a Lorentz profile function depicted in Eq. (3) and in Fig. 1.

$$\Delta f_D = \frac{2 f_{12}}{c}\sqrt{\frac{2kT\ln 2}{m}} \tag{2}$$

$$F_D(f) = \exp\left(-\left(\frac{2(f - f_{12})}{\Delta f_D}\right)^2 \ln 2\right) \tag{3}$$

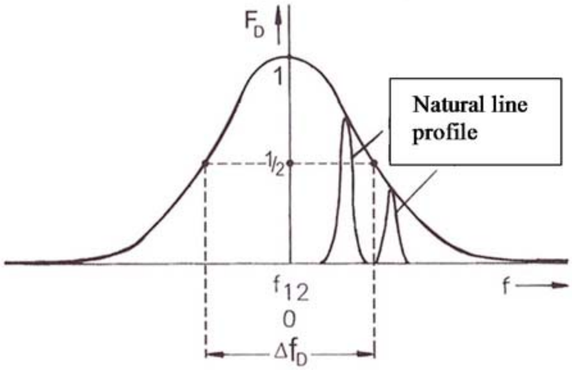

Fig. 1. Doppler broadening.

The half-width for a He-Ne laser is approx. 1.5 GHz, which is far above the natural line width and the collision broadening. In most cases, multiple propagation mechanisms occur at the same time. The natural line width is negligible due to the small proportion. In the case of a gas laser, for example, collision and Doppler broadening mainly occur, with Doppler broadening having the greater part at low pressure, shown in Fig. 2.

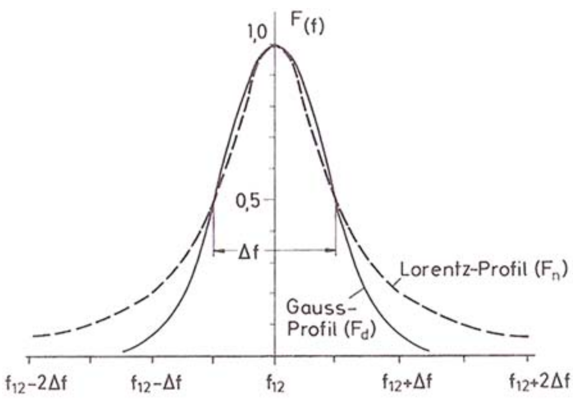

Fig. 2. Line shape functions: Gauss- and Lorentz profile.

With solid-state lasers, a homogeneous broadening occurs due to lattice oscillations or non-homogeneous due to the Stark effect, which describes the shift or splitting of spectral lines in the electric field.

To describe the accuracy of a frequency reference, one refers to the ratio of the relative frequency deviation to the absolute transmission frequency of the atomic or molecular transition used. With the Cesium standard at 10 MHz, a source with an accuracy of 1.5×10^{-14} is available internationally. The second is 9,192,631,770 times the period of the radiation corresponding to the transition between the two hyperfine structure levels of the ground state of atoms of the nuclide ^{133}Cs [4].

Additional standards are available in most developed industrial countries from their respective metrology organizations. Since such a source is only portable to a limited extent, a further secondary source based on the Cs reference is sought. On the one hand, the accuracy of the reference at 10 MHz must be extended to other frequency ranges egg. To realise a frequency comb [5-6].

Starting from the Cs standard with an accuracy of better 10^{-14}, there should be a class of reference lasers in the field of optical communication technology derived directly from the Cs in the overlay experiment. These lasers should have an accuracy of better than 10^{-10}. Building on this, there should be portable laboratory standards that should achieve a frequency accuracy of 10^{-9} (Δf_{or} = 0.2 MHz at f = 200 THz or λ = 1500 nm). The distance between two reference frequencies should not exceed $\Delta\lambda_R$ = 20 nm in order to allow a sufficiently small distance between two calibration points of a spectrometer [7].

Atomic and molecular absorption lines are used in a wide range of optics as a wavelength calibration references, since these form even under fluctuating ambient conditions highly stable frequency standards. Molecules such as acetylene and hydrogen cyanide have very narrow-band absorptions in the range of 1500 nm [1, 8-10]. These transitions can be easily detected directly by absorption spectroscopy. Atomic transitions of rare gases in the range of 1300-1700 nm are generally not directly detectable because they are transitions between excited states of the atom. Usually, these excited states are produced by means of laser excitation or by an electrical gas discharge. A single gas laser reference line from the HeNe laser at 1523 nm is available.

These portable laboratory standards [11] with a frequency accuracy of 10^{-9} (0.2 MHz at 200 THz, 1500 nm) represent an important link between the non-portable reference laser and the less accurate field equipment. These laboratory standards make a very demanding electronics and beam guidance necessary to avoid the Doppler broadening of the natural linewidth of the absorptions used [12-14].

2.1. Opto-galvanic Effect

As soon as a gas discharge is irradiated with light whose photon energy corresponds to the energy of an atomic transition of the discharge, a change in the electrical properties can be observed. A distinction is made between a positive ($\Delta I > 0$) and a negative ($\Delta I < 0$) opto-galvanic effect, depending on the direction of the change in the current intensity. Which of these effects occurs depends on the length of time the electrons stay in the energy levels. In the case of a long-lived higher state, the current increases because more electron-ion pairs are formed in the discharge. In the case of a short-lived state, the probability of ionization decreases and a negative change in current occurs. If these phenomena occur within 100 µs after laser excitation, it is called the slower opto-galvanic effect. With the fast opto-galvanic effect, as occurs with highly excited (Rydberg) atoms, the reaction takes place after less than 1 µs.

With a Galvatron tube, this resonance phenomenon between discharge plasma and laser is used. A laser shines through the ring-shaped cathode of the Galvatron. When the wavelength of laser radiation corresponds to an absorption line, the electrical state of an atom changes as an electron is raised to a higher level. This also changes the number of ions and free electrons present in the plasma. This leads to a reduction in the ionization limit and more atoms can be ionized more easily. By reducing the number of free electrons, the electrical resistance decreases, which can easily be demonstrated with a lock-in amplifier.

This opto-galvanic effect can be used to stabilize the absolute wavelength of a laser. The relevant laser transitions for krypton are shown in Fig. 8. Every energy transition shows a clearly detectable absorption line in the spectrum. E.g. the transition from 5p –> 4d of the wavelength λ = 1533.91577 nm and the transition 5s –> 5p is assigned to the wavelength λ = 1547.8261 nm.

3. Experimental Setup

Fig. 3 and Fig. 4 show the test site with the equipment used. From the tenable laser source (0) the laser beam is modulated by the chopper wheel (1) intensity. The control unit of the chopper is connected to a phase sensitive lock-in amplifier which detects the change in electrical voltage in the Galvatron tube (3). A high voltage supply was used to start the discharge current.

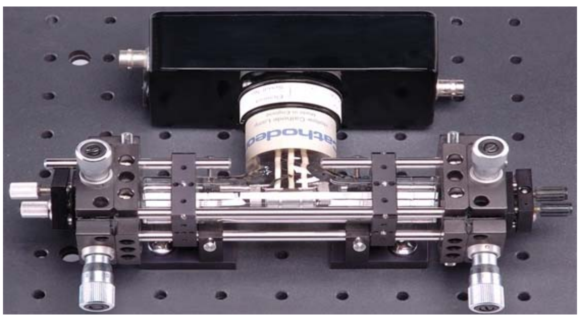

Fig. 3. Experimental setup Galvatron tube with optical coupling setup.

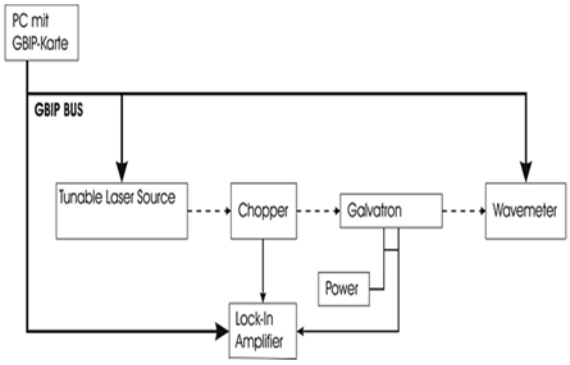

Fig. 4. Electrical and optical connections of experimental setup.

With the wave meter (4) the wavelength is determined with an accuracy of 3×10^{-13}. In the Galvatron-tube, the isotopes of Krypton are included in the following proportions (see Table 1). It also contains as a filling gas Neon, the cathode is made of iron.

In examining the temperature dependency the Galvatron tube was placed in a climate chamber, shown Table 2.

Table 1. Isotopic proportions of natural Krypton gas [14].

Isotope	^{78}Kr	^{80}Kr	^{82}Kr	^{83}Kr	^{84}Kr	^{86}Kr
Part [%]	0,35	2,28	11,59	11,49	57,00	17,30

Fig. 4 shows the schematic setup of and the connections between the devices used. All units were controlled with the help of the GPIB interface of a LabVIEW program that increases the wavelength of the laser source from a start value to an end value with a fixed step size. The intensity of the lock-in amplifier and the wavelength is read at the wave meter and stored in a file. Since the wavelength range could not be covered by a laser source, 3 different sources with the following areas a) were 1270-1375 nm b) 1370-1480 nm, and c) used from 1440 to 1640 nm.

In Fig. 5 and Fig. 6 the measure section is depicted beginning at the laser source via the chopper, the Galvatron-tube to the wave meter. In the experiments, the laser source is operated with an output power of 10 dB, which is lowered by the loss of connectors and especially by the chopper and the Galvatron-tube down to -21 dB at the wave meter.

Table 2. Values of the lines at 1286.54106 nm at various temperatures.

T/ °C	λ [nm]	FW-HM [pm]	λ [nm]	FW-HM [pm]	λ [nm]	FW-HM [pm]
10	1286,53624	2,52	1286,54123	3,0	1286,54583	2,31
20	1286,53619	2,56	1286,54121	3,24	1286,54584	2,33
30	1286,53621	2,58	1286,54120	3,11	1286,54581	2,34
40	1286,53621	2,63	1286,54121	3,12	1286,54582	2,34
50	1286,53623	2,73	1286,54122	3,12	1286,54583	2,45

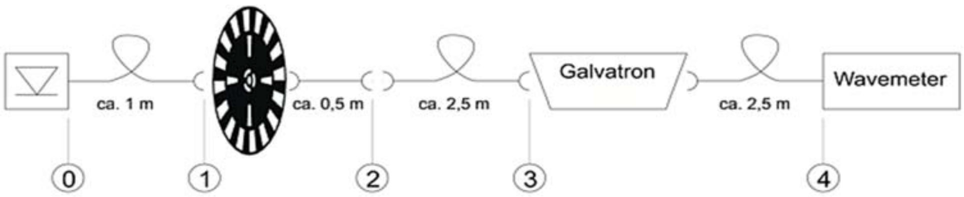

Fig. 5. Optical setup: 0: tenable laser source, 1: optical chopper wheel, 2: opt. connector, 3: Galvatron tube, 4: optical high resolution wave meter.

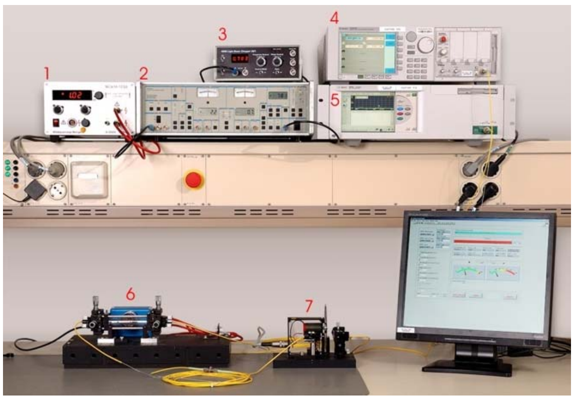

Fig. 6. Photograph of experimental set-up.

Based on the LabVIEW program (see Fig. 6) created by van Doornail [15], some modifications and extensions were made. The entire communication with regard to setting parameters and reading out the measured values from the laser source and the wave meter has already been implemented. The previous program includes a part in which the internal modulation of the laser source was programmed. The internal intensity modulation was not acceptable for our experiment because the distance between the main wavelength and the sidebands was too small. The modulation is implemented externally via a chopper. This reduced the intensity or the spacing of the sidebands that occurred.

Previously, the measured values of the lock-in amplifier were read out via a DAQ card. By converting the GPIB interface of the lock-in amplifier, the measured values could now be read out digitally, which leads to a further reduction in measurement inaccuracies, since the quantization noise of the analogy-digital conversion of the card is eliminated. For this purpose, the initialization and the measured value recorded at the lock-in amplifier were integrated into the program. Furthermore, the clarity of the program was increased by using local variables and the user interface was restructured.

After starting the LabVIEW program (Main.vi) it is necessary to check the parameters of the lock-in amplifier. The GPIB addresses of the devices are already given as default values (4). Then the start and end value for the wavelength, the step size and the number of samples (repeated measurements) per wavelength (5) are set. Based on the settings of the parameters, an estimate of the measurement duration (9) is given. After clicking on “Start” (2) it takes a few seconds for the first measurement to be carried out, then a query (6) appears as to where the data should be saved. The estimation of the measurement duration changes to the remaining time display. For each sample (8) the data of the wave meter (7), the lock-in amplifier (11) and the chopper (12) are read in, displayed and saved. If you click on "ABORT" (3), the measurement of the current step (measurement of a wavelength) is carried out until the end and the program is then ended.

In almost all measurements, the laser source was operated with an output power P = 10 dB (corresponds to 10 maw). Due to line attenuation and losses at plugs, choppers and Galvatron tubes, only approx. –21.1 dB are measured on the wave meter at a wavelength of 1550 nm, which is completely sufficient, since this power is only required for the precise determination of the wavelength.

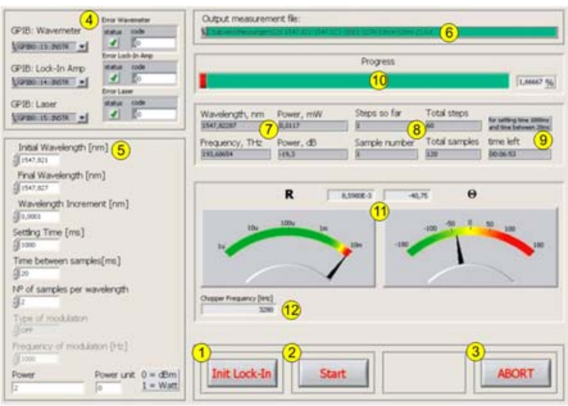

Fig. 7. LabVIEW user interface.

4. Results and Discussion

From Kaufmann, *et al.*, an energy level diagram from Kr I is available which is depicted in Fig. 8. Several absorption lines are can be noticed between 5S and 8S level. Here, the absorption lines of Krypton and Neon in the range of 1270-1640 nm were measured. To our knowledge this is the first continuous measurement and presentation of opto galvanic absorption lines in the whole range of the ITU-T G.652 [16] for optical communication systems. In Fig. 9, there are the consistently numbered absorption lines of Galvatron tube in the areas of laser sources.

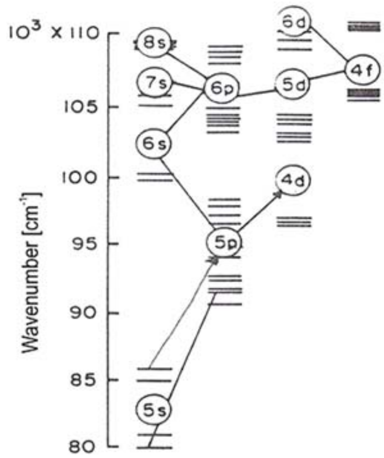

Fig. 8. Excerpt from the energy level diagram of Kr I from [17].

It should be noted, is that lines of neon (eg line 01), iron (eg line 27) and carbon (eg line 15) were measured. These were using the database of the NIST determined [2]. Afterwards, at selected lines ({1286.54123 nm line 03}, {1374.26111 nm line 10} and {1547.82593 nm line 41}) the influence of temperature on the drift of the intensity maximum is investigated. As an example the results of the krypton absorption line shown at 1286.54 nm (Fig. 5d) is depicted. The picture shows the superposition of three isotopes of krypton and the Gaussian fit of the three individual lines. The resulting deviations of the wavelengths from those described in the literature [17-19] are due to the measurement accuracy of the wave meter.

In the tests no drift of the main peak as a function of temperature could be determined (see Table 2). The half-maximum-value width of the main peak remains almost constant. In the secondary maxima a slight broadening was observed with increasing temperature.

5. Conclusions

A complete overview of all opto-galvanic absorption lines of Krypton and Neon mixed gas in the range of ITU-T G.652 were measured and reported. The measured absorption lines show little deviations on the dates given in the literature. The largest deviations were ± 0.5 pm, which can be explained already by the measurement accuracy of the used Agilent wave meter.

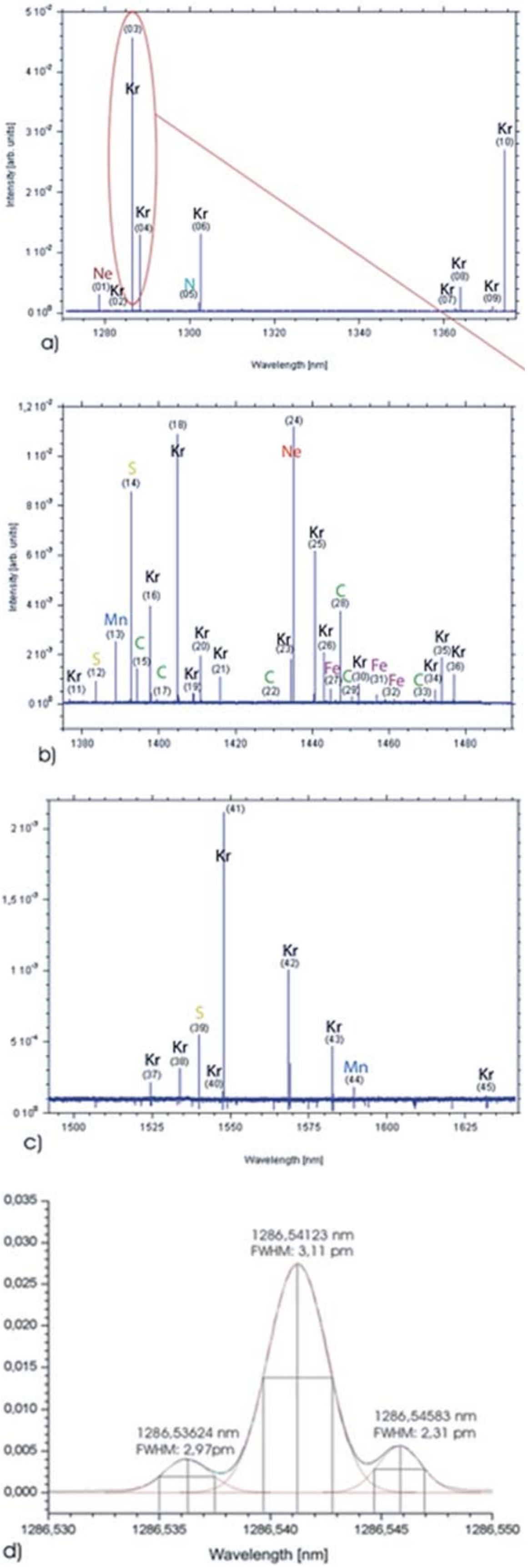

Fig. 9. Absorption lines of Kr line 1286.54123 nm at 10 °C, a) Kr-absorption lines between 1200 nm – 1380 nm, b) Kr-absorption lines between 1380 nm – 1490 nm, c) Kr-absorption lines between 1490 nm – 1640 nm, d) High resolution absorption spectrum Kr 1286 nm-line.

The stronger lines are separated between 5 nm and 30 nm. Hence the creation of a grid of excellent reference lines can be used as a very high precise wavelength standard for optical communications or in spectrum analysers for internal calibration. Since the absorption lines do not depend on the temperature, a long-term stable wavelength standard is technical applicable.

Acknowledgements

Financial support of the Federal Ministry of Research of Germany is grateful acknowledged.

References

[1]. W. C. Gilbert, S. Swann, Acetylene $^{12}C_2H_2$ Absorption Reference for 1510 nm to 1540 nm Wavelength Calibration - SRM 2517a, *NIST Publication*, 2001, Report Number: 260-133.

[2]. Y. Ralchenko, NIST atomic spectra database, *Mem. S.A.It. Suppl.*, Vol. 8, 2005, pp. 96–102.

[3]. M. Poulin, C. Latrasse, N. Cyr, M. Têtu, An absolute frequency reference at 192.6 THz (1556 nm) based on a two-photon absorption line of rubidium at 778 nm for WDM communication systems, *IEEE Photonics Technol. Lett.*, Vol. 9, Issue 12, 1997, pp. 1631–1633.

[4]. PTB, International cesium standard, 2005. [Online]. Available: http://www.ptb.de/de/publikationen/download/zeit_dt.pdf

[5]. E. Benkler, F. Rohde, H. R. Telle, Endless frequency shifting of optical frequency comb lines, *Optscs Express*, Vol. 21, Issue 5, 2013, pp. 5793–5802.

[6]. K. Suzuki, M. Koga, T. Morioka, MHz-accuracy, 25 GHz-spaced frequency-stabilised optical comb over S-, C-, L-bands for precise optical frequency measurements, *Electron. Lett.*, Vol. 40, Issue 17, August 2004, pp. 1078–1079.

[7]. M. Schröder, Wellenlängenstandards für optische Kommunikationssysteme im Bereich 1,2 µm - 1,7 µm, *Harz University of Applied Sciences*, 2013.

[8]. W. C. Swann, S. L. Gilbert, Pressure-induced shift and broadening of 1510–1540-nm acetylene wavelength calibration lines, *Journal of the Optical Society of America B*, Vol. 17, Issue 7, 2000, p. 1263-1270.

[9]. W. C. Swann, S. L. Gilbert, Line centers, pressure shift, and pressure broadening of 1530-1560 nm hydrogen cyanide wavelength calibration lines, *Journal of the Optical Society of America B*, Vol. 22, Issue 8, 2005, p. 1749-1756.

[10]. S. L. Gilbert, W. C. Swann, T. Dennis, Wavelength standards for optical communications, *SPIE*, Vol. 4269, 2001, pp. 184–191.

[11]. U. H. P. Fischer, C. von Helmolt, Engineered, rack-mounted, optical reference unit at 1547.825 nm, *IEEE Photonics Technol. Lett.*, Vol. 6, Issue 11, 1994, pp. 1383–1385.

[12]. A. Gumaste, T. Antony, DWDM Network Designs and Engineering Solutions, *Cisco Systems*, 2002.

[13]. E. Voges, K. Petermann (Hrsg), Optische Kommunikationstechnik – Handbuch für Wissenschaft und Industrie, *Springer-Verlag*, Berlin, 2002, p. 458.

[14]. WebElement, Periodic table on the web: Kr-spectroscopic tables, 2001. [Online]. Available:

http://www.webelements.com/webelements/elements/text/Kr/isot.html.

[15]. M. van Doornik, Bericht zum Projekt praktikum Hochschule Harz, Wernigerode, 2005.

[16]. ITU-T G652, ITU-T G.652 Transmission Systems and Media, Digital Systems and Networks, Transmission media characteristics – Optical fibre cables, *ITU*, 2000.

[17]. C. J. Kaufmann, V. Humphreys, Accurate Energy Levels and Caslculated Wavelengths of 86Kr, *J. Opt. Soc. Am.*, Vol. 59, Issue 12, 1969, pp. 1614-1628.

[18]. U. H. P. Fischer, N. Karlovac, Holographic filter stabilized laser for use as an optical frequency reference for HDWDM systems, *J. Opt. Commun.*, Vol. 20, 1999, pp. 656–658.

[19]. U. H. P. Fischer, M. Schröder, Opto-Galvanic Spectroscopy of Kr 84 / Ne Transitions in the Range of 1270 nm– 1640 nm for use as Optical Wavelength Standards, in *Proceedings of the 2nd IFSA Frequency & Time Conference (IFTC'2020)*, 2020, p. 5192-196.

Published by International Frequency Sensor Association (IFSA) Publishing, S. L., 2020 (http://www.sensorsportal.com).